Plasma and Cerebrospinal Fluid Pharmacokinetics of Erlotinib and Its Active Metabolite OSI-420

Alberto Broniscer,[1] John C. Panetta,[2] Melinda O'Shaughnessy,[2] Charles Fraga,[2] Feng Bai,[2] Matthew J. Krasin,[3] Amar Gajjar,[1] and Clinton F. Stewart[2]

Abstract

Purpose: To report cerebrospinal fluid (CSF) penetration of erlotinib and its metabolite OSI-420.

Experimental Design: Pharmacokinetic measurements were done in plasma (days 1, 2, 3, and 8 of therapy) and, concurrently, in plasma and CSF (before and at 1, 2, 4, 8, and 24 h after dose on day 34 of therapy) in an 8-year-old patient diagnosed with glioblastoma who received local irradiation and oral erlotinib in a phase I protocol. CSF samples were collected from a ventriculoperitoneal shunt, which was externalized because of infection. Erlotinib concentrations were determined by liquid chromatography/mass spectrometry. CSF penetration of erlotinib and OSI-420 were estimated by a compartmental model and by calculating the ratio of CSF to plasma 24-h area under concentration-time curve (AUC_{0-24}).

Results: This patient was assigned to receive erlotinib at a dose level of 70 mg/m^2, but the actual daily dose was 75 mg (78 mg/m^2). Erlotinib and OSI-420 plasma pharmacokinetic variables on days 8 and 34 overlapped to suggest that steady state had been reached. Whereas erlotinib and OSI-420 AUC_{0-24} in plasma on day 34 were 30,365 and 2,527 ng h/mL, respectively, the correspondent AUC_{0-24} in the CSF were 2,129 and 240 ng h/mL, respectively. Erlotinib and OSI-420 CSF penetration were 7% and ~9%, respectively, using both estimate methods. The maximum steady-state CSF concentration of erlotinib was ~130 ng/mL (325 nmol/L).

Conclusions: The plasma pharmacokinetics of erlotinib in this child overlapped with results described in adults. Oral administration of erlotinib achieves CSF concentrations comparable with those active against several cancer cell lines in preclinical models.

Erlotinib hydrochloride (formerly known as OSI-774), an orally administered epidermal growth factor receptor and ERBB2 inhibitor, has been approved in the United States for use in patients with locally advanced or metastatic non–small cell lung cancer and for patients with locally advanced or metastatic pancreatic cancer (1, 2). Erlotinib has also been tested as a single agent in adult patients with several types of cancer, including primary brain tumors (3–8).

Although the pharmacokinetics of erlotinib in both healthy volunteers and adult patients with cancer has been well characterized (6, 9–11), very little is known about the central nervous system penetration and exposure to this drug (12), which is a critical issue in the treatment of patients with primary brain tumors or systemic cancers with predisposition for brain and/or leptomeningeal spread.

We describe for the first time extensive plasma and cerebrospinal fluid (CSF) pharmacokinetics of erlotinib and its active metabolite OSI-420 in one of our patients.

Materials and Methods

This 8-year-old mixed-race female presented with a 3-week history of progressive headaches. After a brain computed tomography showed a left thalamic mass, she underwent surgical resection of the tumor twice and also required ventriculoperitoneal shunt placement for hydrocephalus. She was then referred to our institution for further treatment. Histologic review confirmed the diagnosis of glioblastoma (WHO grade IV). Brain magnetic resonance imaging revealed subtotal resection of the tumor, which involved the left thalamus and midbrain, and enlargement of the left temporal horn of the lateral ventricle. Spine magnetic resonance imaging disclosed no tumor spread. Decompression of her left lateral ventricle was done before initiation of further therapy by insertion of a new catheter into that space, which was connected to the preexisting ventriculoperitoneal shunt.

Adjuvant treatment consisted of the combination of local conformal radiation therapy and erlotinib in a phase I clinical trial for patients between the ages of 3 and 25 years with newly diagnosed high-grade glioma. This clinical trial was approved by the Institutional Review Board at St. Jude Children's Research Hospital. Informed consent for participation on this clinical trial and for plasma pharmacokinetic studies was obtained from the patient's mother and assent was obtained from the patient. Erlotinib therapy was started on the 1st day of

Authors' Affiliations: Departments of [1]Oncology, [2]Pharmaceutical Sciences, and [3]Radiological Sciences, St. Jude Children's Research Hospital, Memphis, Tennessee
Received 9/25/06; revised 11/14/06; accepted 12/12/06.

Grant support: NIH Cancer Center Support (CORE) grant P30 CA21765, American Lebanese Syrian Associated Charities, Noyes Foundation, Ryan McGhee Foundation, Musicians Against Childhood Cancer, and Genentech.

The costs of publication of this article were defrayed in part by the payment of page charges. This article must therefore be hereby marked *advertisement* in accordance with 18 U.S.C. Section 1734 solely to indicate this fact.

Requests for reprints: Alberto Broniscer, Department of Oncology, St. Jude Children's Research Hospital, 332 North Lauderdale, Mail Stop 260, Memphis, TN 38105. Phone: 901-495-4925; Fax: 901-521-9005; E-mail: alberto.broniscer@stjude.org.

doi:10.1158/1078-0432.CCR-06-2372

radiation therapy at a dose of 70 mg/m^2 administered orally once daily. The actual dose of erlotinib was rounded to 75 mg daily (78 mg/m^2). Ondansetron was used as antiemetic throughout the duration of radiation therapy. Dexamethasone was started on day 9 of therapy because of progressive neurologic signs. Ranitidine administration was also started as prophylaxis for the gastrointestinal side effects of dexamethasone. Our patient experienced grade 3 hypophosphatemia and hypokalemia during the 2nd week of therapy, which improved with oral electrolyte supplementation. A CSF leak through the shunt incision, which required shunt externalization, was diagnosed on day 20 of therapy. Intravenous cefazolin was started, but it was later switched to vancomycin because of a positive CSF culture for *Streptococcus viridans*. Erlotinib and local radiation therapy were continued without interruption after shunt externalization. The ventriculoperitoneal shunt was reinternalized once target radiation therapy dose of 59.4 Gy was reached.

Plasma and CSF erlotinib sampling and bioanalysis. Serial plasma samples were collected after the first dose of erlotinib and on day 8 of therapy. Erlotinib dose was held on day 2 in all patients where consent was obtained for pharmacokinetic studies. Two milliliters of blood were drawn before and at 1, 2, 4, 8, 24 (±2), 30 (±4), and 48 (±4) h after the first dose of erlotinib and before and at 1, 2, 4, 8, and 24 (±2) h after the erlotinib dose on day 8.

At the time of ventriculoperitoneal shunt externalization, we obtained additional Institutional Review Board approval to do serial, concurrent plasma and CSF pharmacokinetic studies. Once appropriate consent was obtained, 2 mL of blood were drawn simultaneously with CSF samples before and at 1, 2, 4, 8, and 24 h after erlotinib administration on day 34 of therapy. Each CSF collection was conducted in a sterile manner by allowing free flow of CSF under gravity over intervals between 6 and 12 min. Between 0.3 and 2.0 mL of CSF were obtained with each collection. To determine the approximate flow rate through the externalized shunt tubing, the volume of CSF that drained between each sample collection was also determined. Flow rate was determined by dividing the volume of CSF by the span of time over which it was collected.

Plasma and CSF erlotinib and OSI-420 concentrations were determined by a validated liquid chromatography/mass spectrometry method (13). The internal standard used was CP-396,059. Erlotinib and OSI-420 were extracted from plasma and CSF using 3 mL t-butyl methyl ether followed by shaking for 10 min and centrifugation for 10 min. The organic layer was transferred to a clean tube and evaporated to dryness. The dried extract was reconstituted in 200 μL of 80% methanol/water. Fifteen microliters of the reconstituted sample were directly injected into the liquid chromatography/mass spectrometry system. Chromatographic separation was achieved by gradient elution on a Phenomenex Luna 3μ C18 (50 × 4.6 mm; Phenomenex, San Francisco, CA). The mobile phase consisted of 80% methanol and 20% NH_4COOH (10 mmol/L) at a pH of 4.8. Compound detection was accomplished by chemical ionization at atmospheric pressure on an API 3000 (Applied Biosystems, Toronto, Ontario, Canada). The plasma standard curves, which ranged from 10 to 2,500 ng/mL for erlotinib and from 1 to 700 ng/mL for OSI-420, were fitted to a 1/×-weighted regression model. The CSF standard curves, which ranged from 1 to 250 ng/mL for erlotinib and from 0.1 to 70 ng/mL for OSI-420, were also fitted to a 1/×-weighted regression model. The lower limit of quantification for erlotinib and OSI-420 was 0.2 ng/mL. Control samples to assess the accuracy and precision of the assay were measured along with the study samples. Values for the between-run and within-run precision were <6.8% and <5.9% of the coefficient of variation, respectively, with deviations from the nominal concentrations of ±9.2%.

Compartmental pharmacokinetic modeling of plasma and CSF erlotinib and OSI-420. The pharmacokinetics of erlotinib and OSI-420 in both plasma and CSF were determined using the compartmental model depicted in Fig. 1. This model has a gut compartment, a central and peripheral plasma compartment, and a single CSF compartment for both erlotinib and OSI-420. Additionally, a delay (Tau) between the gut and plasma compartments and a second delay between the plasma and CSF compartments were incorporated. The second delay was added to account for the time (82 min) that it took for the CSF to flow through the shunt tubing (volume of 6.6 mL). The rate variables are defined as follows: k_a, the absorption rate from the gut; k_e, the conversion of erlotinib to OSI-420; k_{emet}, the elimination rate of OSI-420; and k_{23} and k_{32}, and k_{45} and k_{54}, the influx and efflux rates between the plasma and CSF for erlotinib and OSI-420, respectively. All rate variables have the unit of HR^{-1}. Additionally, V / F is the apparent volume of distribution of the erlotinib plasma compartment, V_{met} / F_{met} is the apparent volume of distribution of the OSI-420 plasma compartment, and V_{CSF} represents the volume of erlotinib and OSI-420 CSF compartment. All volume units are described in liters. Because V_{met} is not identifiable, we set it equal to V. We used an approximate volume of intraventricular CSF of 0.023 L following standard volumes established based on gender and age because V_{CSF} could not be measured for our patient (14). Furthermore, the following secondary variables were determined: erlotinib clearance, $CL = k_eV$; erlotinib CSF penetration (formation/elimination), $k_{23}V$ / $k_{32}V_{CSF}$; and OSI-420 CSF penetration (formation/elimination), $k_{45}V_{met}$ / $k_{54}V_{CSF}$. The CSF penetration was also determined by comparing the ratio of CSF with plasma area under concentration-time curve (AUC), where the AUC for each component was determined using both the model-fitted curve and noncompartmental analysis. The measures of penetration were expressed as a percentage. The model variables were estimated using the maximum likelihood variable estimation method as implemented in ADAPT II (15).

Noncompartmental analysis of plasma and CSF erlotinib and OSI-420 concentrations. As another approach to determine the CSF penetration of erlotinib and OSI-420, we also calculated plasma and CSF AUC values from time 0 to 24 h (AUC_{0-24}) for erlotinib and OSI-420 using a log-linear trapezoidal approach. The ratios of CSF to plasma AUC_{0-24} values for erlotinib and OSI-420 were also expressed as a percentage.

Results

CSF pharmacokinetic studies were done at a time when the CSF cellularity was within normal limits and cultures were

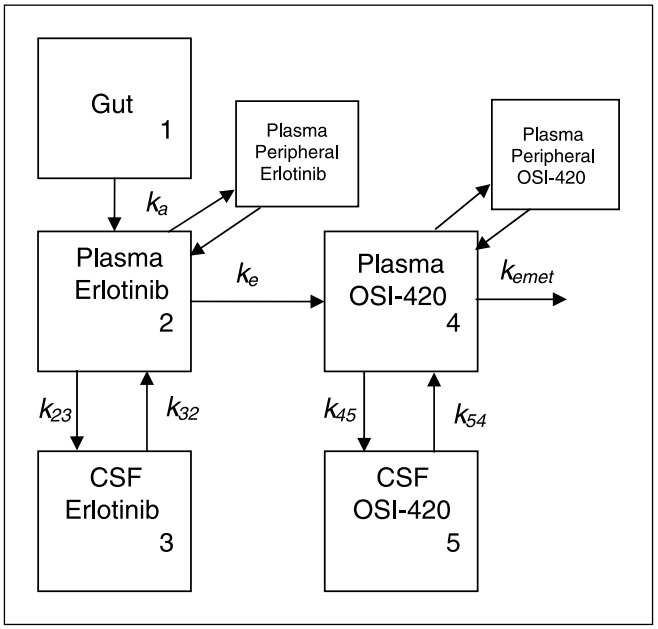

Fig. 1. Compartmental pharmacokinetic model for erlotinib and OSI-420.

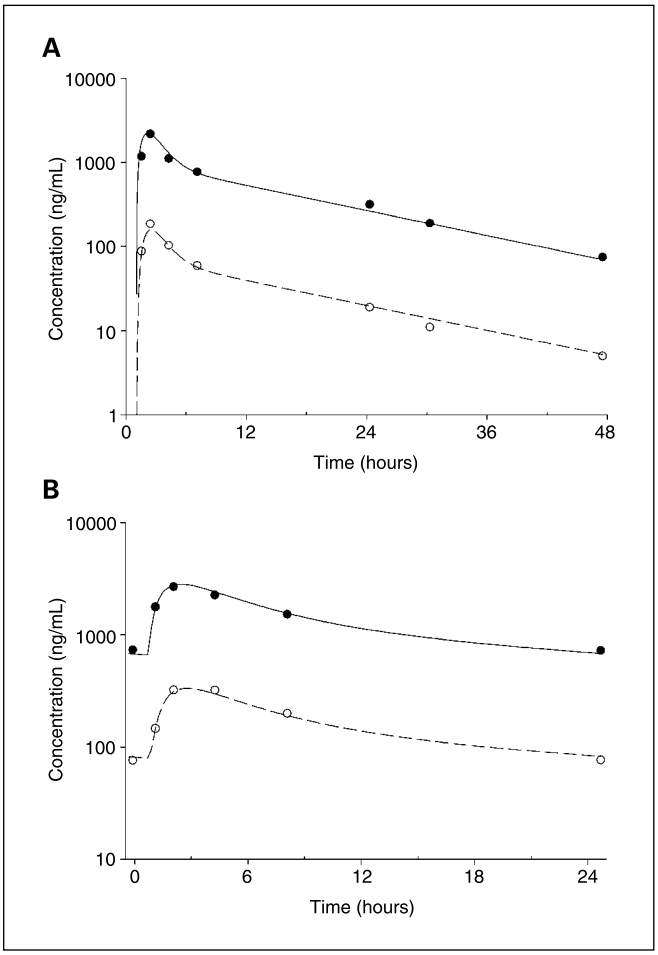

Fig. 2. Plasma concentration-time plots of erlotinib (*solid lines* and *solid circles*) and OSI-420 (*dashed lines* and *open circles*) after days 1 (*A*) and 8 (*B*) of therapy. Circles, the measured plasma concentrations; lines, the best-fit lines from the pharmacokinetic analysis.

already negative. CSF collection was well tolerated and was done without complications. Once the ventriculoperitoneal shunt was reinternalized, this child did not experience any further related complications. Our patient developed grade 2 rash at the time of CSF collection, which remained stable until the discontinuation of erlotinib at week 20 of therapy.

Figure 2 provides the plasma concentration-time plots of erlotinib and OSI-420 after the first dose (Fig. 2A) and on day 8 of therapy (Fig. 2B). The pharmacokinetic variables, including the intercompartment rate constants, half-lives, and apparent volumes of distribution determined after the first dose and on days 8 and 34 of erlotinib administration are summarized in Table 1.

Figure 3 depicts the plasma and CSF concentration-time plots of erlotinib and OSI-420 on day 34 of therapy. The disposition of erlotinib in the plasma on day 34 was similar to that observed on day 8 (oral clearance of 23.7 versus 25.9 L/h/m^2 for days 8 and 34, respectively; Table 1), indicating that this patient had reached steady state when the CSF studies were done.

The CSF penetration of erlotinib and OSI-420 calculated using the compartmental model were 7.0% and 9.5%, respectively. Because the CSF concentration of the samples obtained before and 24 h after erlotinib administration on day 34 did not fit well into the curve drawn based on the compartmental model (Fig. 3), we considered several alternatives to better describe the distribution of these samples (data not shown), including a nonlinear model that took into account the possible influence of erlotinib concentration on the transport between the plasma and CSF compartments. Because these variations in the model did not improve the fit, we also used a noncompartmental approach to determine the CSF penetration of erlotinib and OSI-420. The CSF penetration of erlotinib and OSI-420 were 6.9% and 8.6%, respectively, based on the ratio of the respective CSF and plasma AUC_{0-24} (Table 1). The erlotinib CSF concentrations 4 and 8 h after dosage on day 34 of therapy were 129 ng/mL (322.5 nmol/L) and 139 ng/mL (347.5 nmol/L), respectively (Fig. 3).

Discussion

We showed for the first time that the oral administration of erlotinib yields CSF concentrations comparable with those that were shown to be active in preclinical studies. In our patient, the maximum steady-state CSF concentrations of erlotinib were reached between 4 and 8 h after drug administration and were ~130 ng/mL (325 nmol/L). As a comparison, multiple studies have reported inhibitory effects of erlotinib against several tumor cell lines *in vitro*, including those derived from colorectal, head and neck, breast, and lung cancer, and medulloblastoma at concentrations similar to those reached in the CSF in our patient (16–18). Although OSI-420 retains antitumor activity, its concentration in the CSF represented only 10% of that of erlotinib in our patient.

Consistent with a phase I study design, our patient received a dose of erlotinib that was 10% lower than the recommended dose for phase II studies in adults (9) and almost one third

Table 1. Summary of pharmacokinetic variables for erlotinib and OSI-420

Variable	Day 1 (CV%)	Day 8 (CV%)	Day 34 (CV%)
CL (L/h/m^2)	37.9 (4)	23.7 (5)	25.9 (6)
K_a (h^{-1})	0.94 (43)	0.24 (59)	0.17 (145)
K_e (h^{-1})	0.29 (52)	0.49 (72)	0.29 (142)
K_{emet} (h^{-1})	3.96 (52)	4.07 (71)	3.46 (141)
Tau gut (h)	1.05 (14.4)	0.74 (21)	0.0 (Fixed)
Tau CSF (h)			1.37 (Fixed)
K_{23} (h^{-1})			1.02×10^{-4}
K_{32} (h^{-1})			6.00
K_{45} (h^{-1})			0.98×10^{-4}
K_{54} (h^{-1})			4.79
V (L/m^2)	13.1 (52)	4.87 (73)	9.02 (145)
V_{CSF} (L/m^2)			0.023 Fixed
Erlotinib AUC_{0-24} (ng•h/mL)	19,412	32,851	Plasma, 30,365; CSF, 2,129
OSI-420 AUC_{0-24} (ng•h/mL)	1,416	3,921	Plasma, 2,527; CSF, 240
Erlotinib AUC_{0-24} (ng•h/mL), NCA			Plasma, 28,388; CSF, 1,949
OSI-420 AUC_{0-24} (ng•h/mL), NCA			Plasma, 2,425; CSF, 209

Abbreviations: CV, coefficient of variation; NCA, noncompartmental analysis; CL, oral clearance.

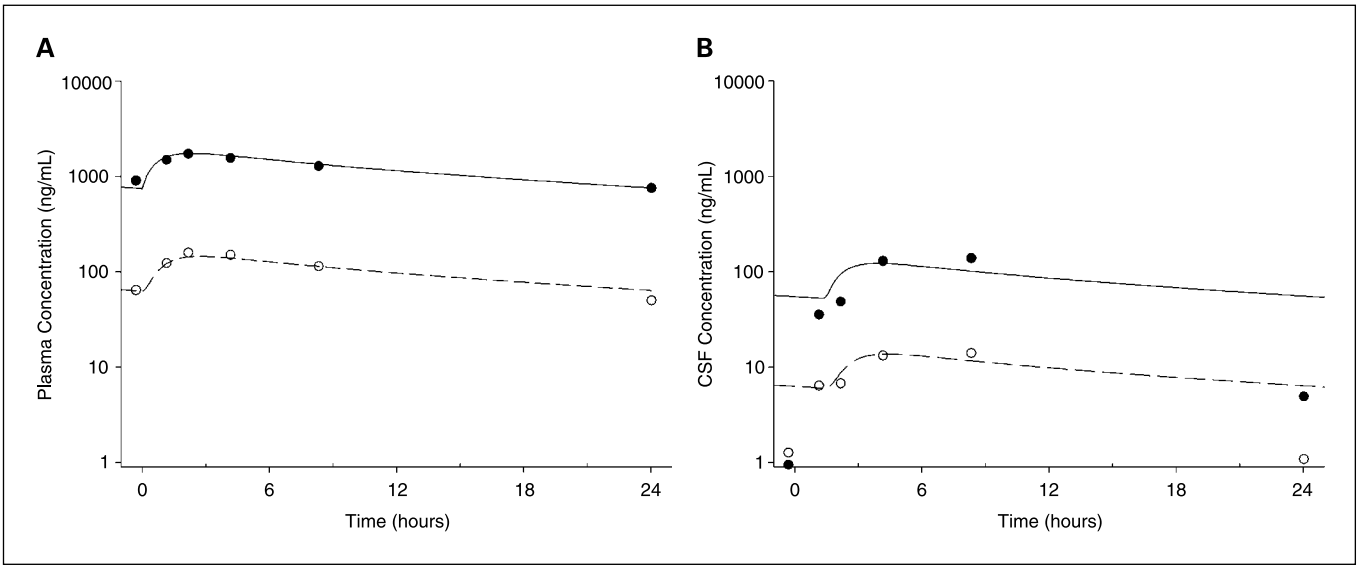

Fig. 3. Plasma (*A*) and CSF (*B*) concentration-time plots for erlotinib (*solid lines* and *solid circles*) and OSI-420 (*dashed lines* and *open circles*) on day 34 of therapy. Circles, the measured concentrations; lines, the best-fit lines from the pharmacokinetic analysis.

lower than the equivalent dose recommended for adults with malignant gliomas not receiving enzyme-inducing anticonvulsants (6). Therefore, higher CSF concentrations of erlotinib would be expected at higher dosage levels, assuming that CSF penetration of erlotinib does not saturate.

Only one previously published study addressed the issue of erlotinib penetration into the central nervous system (12). Lassman et al. described erlotinib and OSI-420 steady-state trough concentrations in tumor samples obtained 24 h after dosing in six patients who underwent surgical resection of recurrent or progressive glioblastoma. These patients had received erlotinib for 1 week at a dose of 150 mg daily before surgery. The steady-state tumor trough concentrations of erlotinib and OSI-420 in four of these six patients were 6% to 8% and 5% to 11%, respectively, of concomitant plasma concentrations. Concomitant pharmacodynamic analysis of phosphorylated epidermal growth factor receptor, AKT, and extracellular signal-regulated kinase by Western blot was done in these four tumor samples and no consistent association of erlotinib therapy with either clinical outcome or status of the above putative targets was observed. In the two remaining patients, the steady-state trough tumor concentrations of erlotinib were 50% and 19% of concomitant plasma concentrations, and the respective OSI-420 concentrations were 54% and 28% of concomitant plasma concentrations. However, in both instances, the pharmacokinetic results were believed to be spurious because the tissue aliquot for pharmacokinetic studies was contaminated with a blood clot, and the respective Western blot analysis showed high phosphorylated epidermal growth factor receptor in both tumors. Overall, erlotinib penetration into four of these tumors was within the range seen in the CSF of our patient. Because the blood-brain barrier is commonly disrupted in high-grade gliomas, it would be reasonable to assume that erlotinib penetration would be higher within these tumors than in CSF. However, further studies will be required to elucidate this issue.

Although erlotinib alone or in combination has been extensively used in the treatment of several different types of cancer originating outside the central nervous system in adults, particularly non–small cell lung cancer (2–5, 7–10), only one case report to date has described activity of this agent in a patient with non–small cell lung cancer and brain metastases (19). Conversely, several case reports and series of patients have described the activity of gefitinib, a very similar oral epidermal growth factor receptor inhibitor, in patients with non–small cell lung cancer and brain metastases, particularly those harboring tumors with mutations in the tyrosine kinase domain of *epidermal growth factor receptor* (20–22).

Three studies to date have described the use of erlotinib alone or in combination in the treatment of adults with primary brain tumors (6, 23, 24). Prados et al. (6) recently reported modest activity of erlotinib when administered with or without temozolomide in adults with recurrent or progressive high-grade glioma. In this study, 8 of 57 evaluable patients, including 5 patients with glioblastoma, had a partial response to therapy. Six of eight patients who experienced radiologic response received erlotinib only, and two patients received erlotinib and temozolomide. However, only two of eight patients had not experienced further tumor progression at the time of publication. The other two studies reported limited experience of erlotinib in combination with radiation therapy in a phase I setting (23) and a retrospective review of radiologic responses in 17 patients who received erlotinib and sirolimus (24).

We cannot draw any conclusions about the role of erlotinib in the therapy of our patient. Despite the modest activity of erlotinib in adults with recurrent high-grade glioma (6), those results are encouraging because of the lack or low activity of other agents in the same setting, including gefitinib (25, 26). The results of ongoing trials, including our own pediatric study, will hopefully elucidate the role of erlotinib in the treatment of patients with primary brain tumors or other systemic cancers with predisposition for central nervous system spread.

References

1. Johnson JR, Cohen M, Sridhara R, et al. Approval summary for erlotinib for treatment of patients with locally advanced or metastatic non-small cell lung cancer after failure of at least one prior chemotherapy regimen. Clin Cancer Res 2005;11:6414–21.
2. Shepherd FA, Rodrigues Pereira J, Ciuleanu T, et al. Erlotinib in previously treated non-small-cell lung cancer. N Engl J Med 2005;353:123–32.
3. Soulieres D, Senzer NN, Vokes EE, Hidalgo M, Agarwala SS, Siu LL. Multicenter phase II study of erlotinib, an oral epidermal growth factor receptor tyrosine kinase inhibitor, in patients with recurrent or metastatic squamous cell cancer of the head and neck. J Clin Oncol 2004;22:77–85.
4. Philip PA, Mahoney MR, Allmer C, et al. Phase II study of erlotinib (OSI-774) in patients with advanced hepatocellular cancer. J Clin Oncol 2005;23:6657–63.
5. Gordon AN, Finkler N, Edwards RP, et al. Efficacy and safety of erlotinib HCl, an epidermal growth factor receptor (HER1/EGFR) tyrosine kinase inhibitor, in patients with advanced ovarian carcinoma: results from a phase II multicenter study. Int J Gynecol Cancer 2005;15:785–92.
6. Prados MD, Lamborn KR, Chang S, et al. Phase 1 study of erlotinib HCL alone and combined with temozolomide in patients with stable or recurrent malignant glioma. Neuro-oncol 2006;8:67–78.
7. Townsley CA, Major P, Siu LL, et al. Phase II study of erlotinib (OSI-774) in patients with metastatic colorectal cancer. Br J Cancer 2006;94:1136–43.
8. Philip PA, Mahoney MR, Allmer C, et al. Phase II study of erlotinib in patients with advanced biliary cancer. J Clin Oncol 2006;24:3069–74.
9. Hidalgo M, Siu LL, Nemunaitis J, et al. Phase I and pharmacologic study of OSI-774, an epidermal growth factor receptor tyrosine kinase inhibitor, in patients with advanced solid malignancies. J Clin Oncol 2001;19:3267–79.
10. Tan AR, Yang X, Hewitt SM, et al. Evaluation of biologic end points and pharmacokinetics in patients with metastatic breast cancer after treatment with erlotinib, an epidermal growth factor receptor tyrosine kinase inhibitor. J Clin Oncol 2004;22:3080–90.
11. Ling J, Johnson KA, Miao Z, et al. Metabolism and excretion of erlotinib, a small molecule inhibitor of epidermal growth factor receptor tyrosine kinase, in healthy male volunteers. Drug Metab Dispos 2006; 34:420–6.
12. Lassman AB, Rossi MR, Raizer JJ, et al. Molecular study of malignant gliomas treated with epidermal growth factor receptor inhibitors: tissue analysis from North American Brain Tumor Consortium Trials 01-03 and 00-01. Clin Cancer Res 2005;11:7841–50.
13. Zhao M, He P, Rudek MA, Hidalgo M, Baker SD. Specific method for determination of OSI-774 and its metabolite OSI-420 in human plasma by using liquid chromatography-tandem mass spectrometry. J Chromatogr B Analyt Technol Biomed Life Sci 2003; 793:413–20.
14. Xenos C, Sgouros S, Natarajan K. Ventricular volume change in childhood. J Neurosurg 2002;97:584–90.
15. D'Argenio DZ, Schumitzky A. ADAPT II User's Guide, University of Southern California. Los Angeles: Biomedical Simulation Resource; 1990.
16. Moyer JD, Barbacci EG, Iwata KK, et al. Induction of apoptosis and cell cycle arrest by CP-358,774, an inhibitor of epidermal growth factor receptor tyrosine kinase. Cancer Res 1997;57:4838–48.
17. Hernan R, Fasheh R, Calabrese C, et al. ERBB2 up-regulates S100A4 and several other prometastatic genes in medulloblastoma. Cancer Res 2003;63: 140–8.
18. Amann J, Kalyankrishna S, Massion PP, et al. Aberrant epidermal growth factor receptor signaling and enhanced sensitivity to EGFR inhibitors in lung cancer. Cancer Res 2005;65:226–35.
19. Lai CS, Boshoff C, Falzon M, Lee SM. Complete response to erlotinib treatment in brain metastases from recurrent NSCLC. Thorax 2006;61:91.
20. Ceresoli GL, Cappuzo F, Gregorc V, Bartolini S, Crino L, Villa E. Gefitinib in patients with brain metastases from non-small-cell lung cancer: a prospective trial. Ann Oncol 2004;15:1042–7.
21. Lee DH, Han JY, Lee HG, et al. Gefitinib as a first-line therapy of advanced or metastatic adenocarcinoma of the lung in never-smokers. Clin Cancer Res 2005;11: 3032–7.
22. Shimato S, Mitsudomi T, Kosaka T, et al. EGFR mutations in patients with brain metastases from lung cancer: association with the efficacy of gefitinib. Neuro-oncol 2006;8:137–44.
23. Krishnan S, Brown PD, Ballman KV, et al. Phase I trial of erlotinib with radiation therapy in patients with glioblastoma multiforme: results of North Central Cancer Treatment Group protocol N0177. Int J Radiat Oncol Biol Phys 2006;65: 1192–9.
24. Doherty L, Gigas DC, Kesari S, et al. Pilot study of the combination of EGFR and mTOR inhibitors in recurrent malignant gliomas. Neurology 2006;67: 156–8.
25. Wong ET, Hess KR, Gleason MJ, et al. Outcomes and prognostic factors in recurrent glioma patients enrolled onto phase II clinical trials. J Clin Oncol 1999;8:2572–8.
26. Rich JN, Reardon DA, Peery T, et al. Phase II trial of gefitinib in recurrent glioblastoma. J Clin Oncol 2004; 22:133–42.

Clinical Cancer Research

Plasma and Cerebrospinal Fluid Pharmacokinetics of Erlotinib and Its Active Metabolite OSI-420

Alberto Broniscer, John C. Panetta, Melinda O'Shaughnessy, et al.

Clin Cancer Res 2007;13:1511-1515.